Mixed Signals
Radio Astronomy Laboratory

Andrew Sheridan Sharks In Space Professor Aaron Parsons

February 7, 2018

Abstract

The purpose of this lab is to gain familiarity with the laboratory equipment and foundational analysis techniques utilized in modern radio astronomy. We focus on the consequences of the Nyquist criterion and the uses of the Fourier transform in signal analysis. By generating a single sine wave at various frequencies and reviewing the sampled signals we confirm that the Nyquist frequency is in fact one half of the sampling frequency. By understanding the Nyquist criterion we demonstrate the ability to record signals at frequencies in excess of those our equipment is technically able to capture. In addition, we construct heterodyne mixers and examine their properties. By demonstrating an understanding of the limitations and strengths of digitally sampled signals as well as the properties of the heterodyne mixer we show our readiness to progress further into radio astronomy.

Introduction

When an electromagnetic wave intersects with a length of wire a voltage potential may be induced. A measurement of this potential provides data about the wave. This straightforward principle allows for measurements of the electromagnetic spectrum.

Devices of this nature began to be employed over one century ago, and when directed towards the heavens we call these devices Radio Telescopes. Over time these devices became more complex and sophisticated, today radio telescopes are paired with fast digital sampling systems. These generate vast amounts of data which are analyzed with modern techniques. To gain an understanding of these systems we review digital sampling, Fourier transforms, and heterodyne mixers.

1 The Nyquist Criterion

1.1 Signal Sampling Method

The sampling equipment in the lab is the PICO Technology PicoScope 2000 Series. Using the pico.read_socket function from the labs homegrown ugradio Python package [1], the sampler has a configurable sampling rate of $(62.5/N)$ MHz, for $N \in \mathbb{Z}$. Our signal generator is the Stanford Research Systems DS340 15MHz Synthesized Function Generator. This combination of devices dictates that our choice of N be at most 5.

Table 1: Generated Signal Frequencies

$\nu_{sig}\ [MHz]$	1.25	2.50	3.75	5.00	6.25	7.50	8.75	10.00	11.25

To examine a broad range of frequencies, we sample at a rate of $\nu_{samp} = 12.5$ MHz. To avoid saturating the Analog-to-Digital converter in the sampler, we generate the signals listed in Table 1 at $0.8V_{p-p}$, and use the pico.read_socket function with a setting of $1V$. The data captured from the sampler is spread over a signed 16bit integer bit-space. As such, it must be scaled by the maximum value of that bit-space. Additionally, we convert the data from Volts to millivolts.

While collecting data, we compare the trace shown on the Textronix 2465 300MHz Oscilloscope to plots of our data to confirm we are getting good readings. In doing so we discover that occasionally the sampler reports incorrect results in the first few elements of the initial block of data. These invalid datum were ignored in our analysis.

[1] Most ugradio functions were employed before the recent update to the package

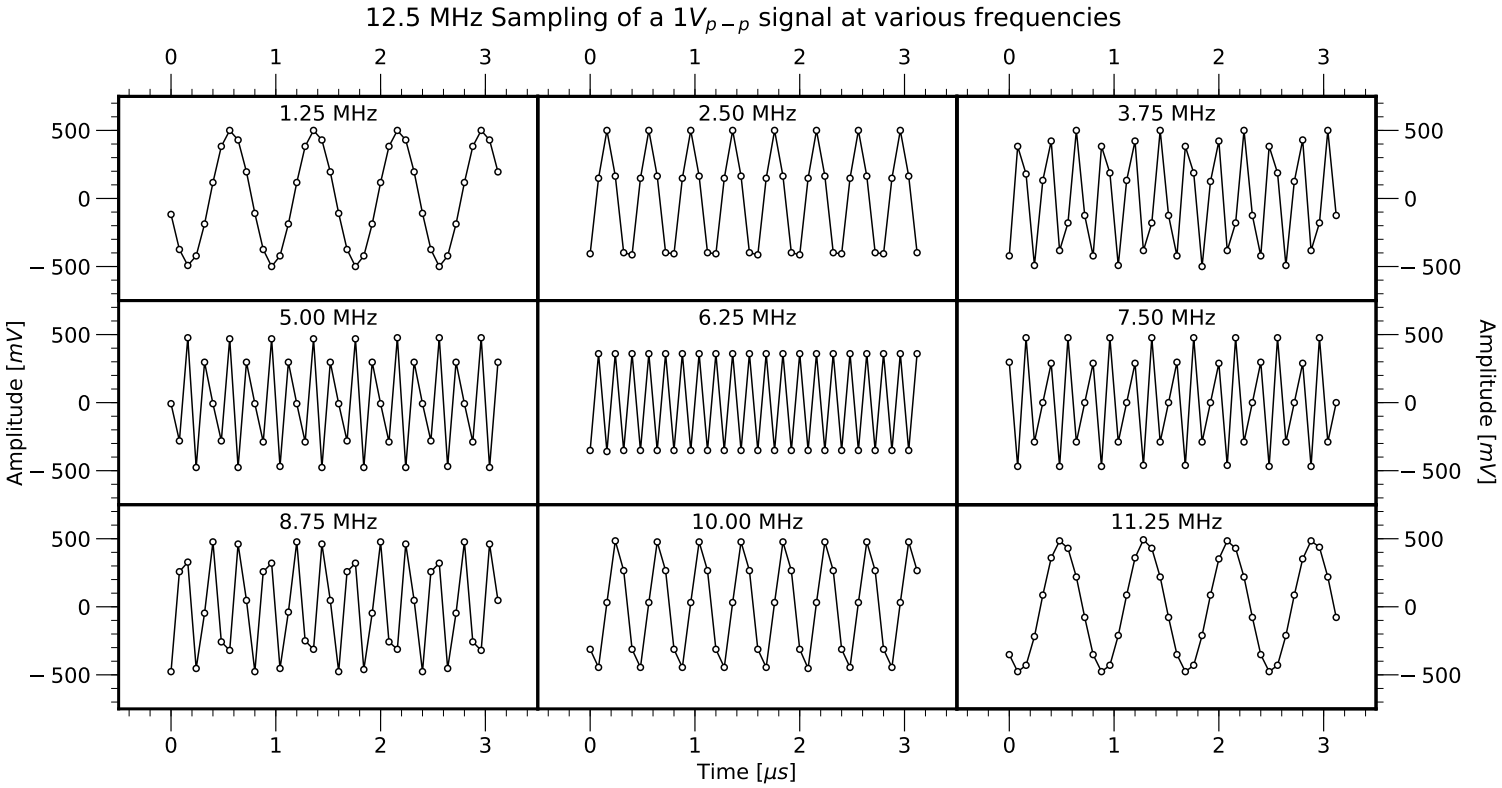

Figure 1: Aliasing in the time spectrum

1.2 The Nyquist Frequency in the Time Series

For each of the frequencies in Table 1 we extract a representative portion of the captured data and present this portion in Figure 1. In each subplot the frequency increases by 1.25 MHz. The central plot shows a signal at 6.25 MHz, the exact frequency at which we sample. Here we see the same signal amplitude repeatedly, and the exact expected number of peaks in the signal is represented. At and below this frequency, the period of the sampled signal matches the period that is expected from its frequency. For signals generated at frequencies larger than 6.25 MHz, something unusual occurs. Higher frequencies appear as lower frequencies. In fact, these signals appear to be inverted mirror images of their lower frequency counterparts.

This phenomena is an example of signal aliasing. When sampling at frequencies higher than $\nu_{samp}/2$, higher frequencies signals appear to be lower frequency signals. This implies that in order to accurately retrieve our signal we must be sure to sample at least at twice the rate of our signal frequency. This special frequency of one half the sampling rate is known as the Nyquist frequency.

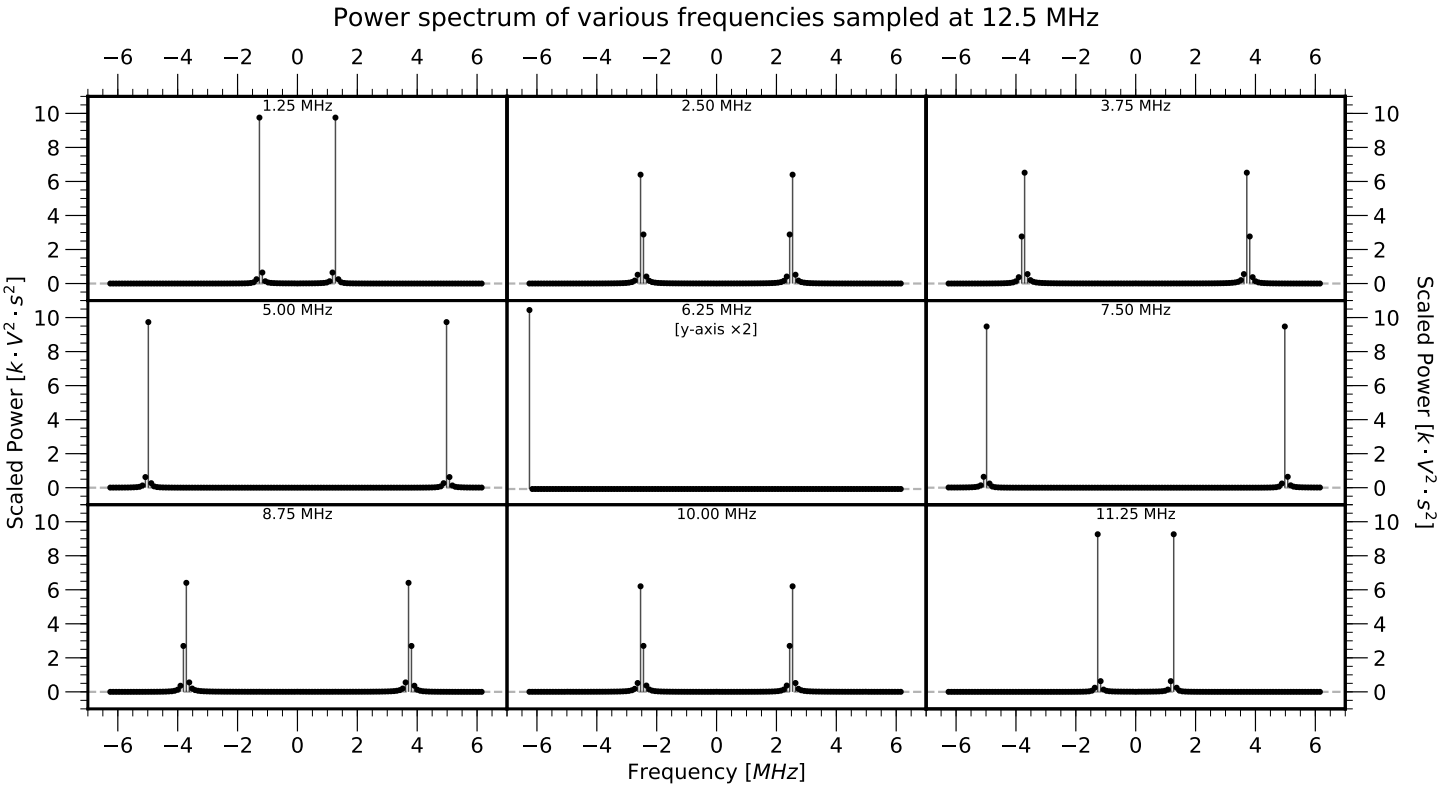

Figure 2: Aliasing in Power Spectra

1.3 The Nyquist Frequency in the Power Spectrum

For each signal in Figure 1 we extract a representative portion[2] of the captured data and perform a discrete Fourier transform using the dft.dft function from the ugradio package. From that transformed data the power spectra are computed by taking the square of their absolute value. In Figure 2 we see a similar effect as witnessed in the time series visualization. The central plot shows the spectrum at 6.25 MHz, the Nyquist frequency. At and below this frequency the plus or minus value of the true frequency of the signal is shown. Each of the recorded frequency for signals above the Nyquist frequency are recorded as $\nu_{samp} - \nu_{sig}$. Above the Nyquist frequency aliasing has caused the power spectra to be reflected back to a frequency other than its true value.

For example, the 10.00 MHz signal is displayed as a 2.5 MHz signal: 12.5 MHz - 10MHz = 2.5 MHz. Understanding this phenomena will allow us to measure signals well beyond the capabilities of our equipment.

[2]Each portion consists of 2^7 elements

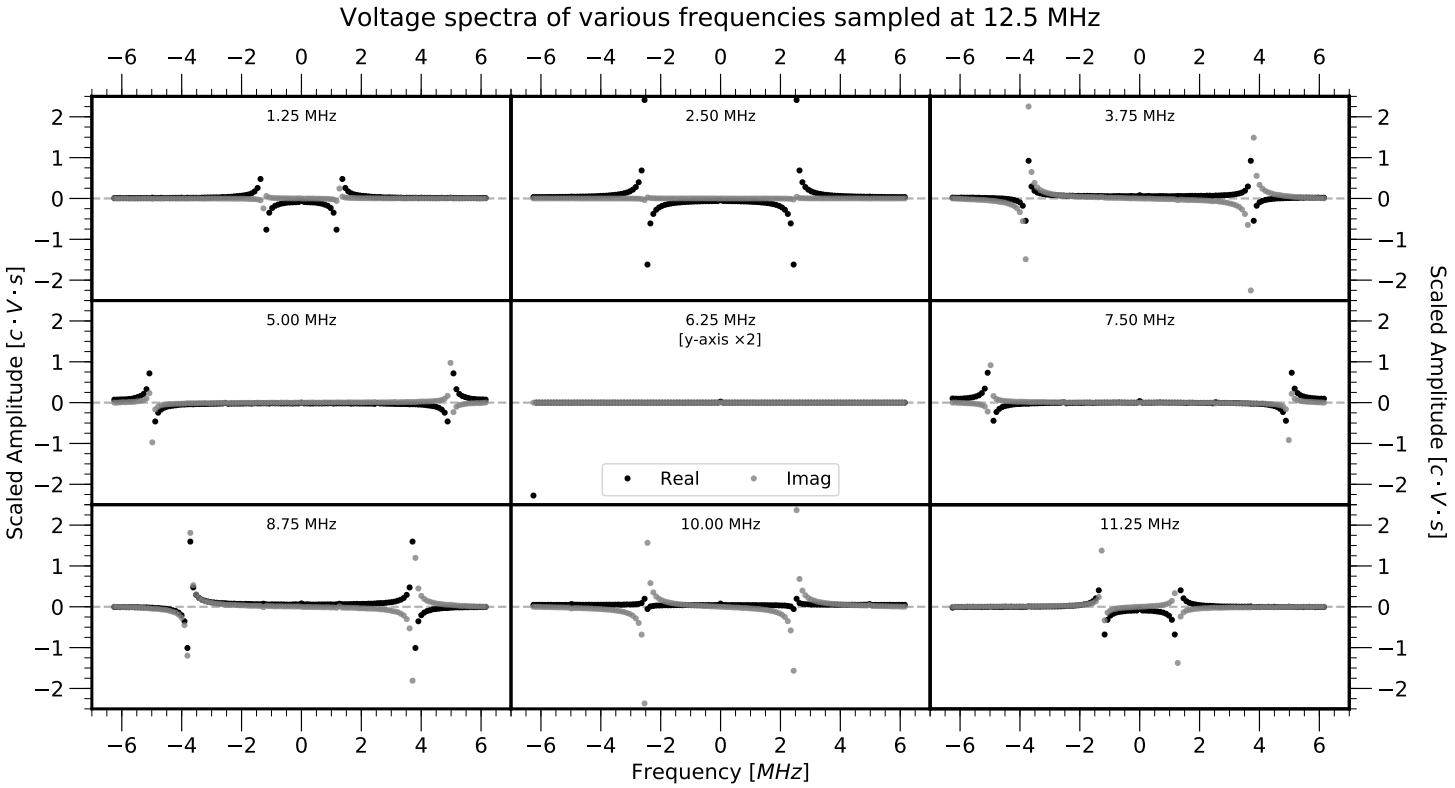

Figure 3: Voltage spectra demonstration of the Nyquist frequency

1.4 Aliasing in Voltage spectra.

For each of the signals in Figure 1 we take the previously computed Fourier transform and separately plot their real and imaginary voltage spectra in Figure 3. As before we see the now familiar reflections caused by the disparity between the sampling rate and the signal frequency, this time with a twist. While the real values are reflected symmetrically about the 0 frequency point, the imaginary values are reflected anti-symmetrically. Additionally, when comparing plots spaced symmetrically from the central plot, we see that the amplitudes of the sin and cosine appear to have switched. Section 2 covers this behavior.

2 Frequency Space

When viewing the voltage spectra in Figure 3 we see how the imaginary data appears to follow different rules than their real counterparts. This behavior in the data is generated by the Fourier transform itself. The Fourier transform is the integral[1]

$$E(\nu) = \frac{1}{T}\int_{-T/2}^{T/2} E(t)e^{2\pi i\nu t}dt$$

2.1 Understanding the Voltage Spectra

Multiplication of the real values time series by the complex exponential ensures that the output of the transform is complex. This explains the presence of real and imaginary components in Figure 3. A closer look will reveal the reason for both the disparity between the real and imaginary magnitudes, as well as the anti-symmetric behavior displayed. The complex exponential is

$$e^{2\pi i(\pm\nu)t} = \cos(2\pi\nu t) \pm i\sin(2\pi\nu t)$$

As ν varies, the sign of the trigonometric terms will alternate in their typical manner, explaining why the magnitudes of the real and imaginary values may be either positive or negative. For any particular ν, switching from positive to negative will cause the sign of the sine term to flip, while the sign of the cosine term will not. This Hermitian symmetry explains why the imaginary values display anti-symmetric behavior around the zero frequency point.

2.2 Understanding the Power Spectra

To compute the power spectrum for a Fourier transform, we multiply the transform by its complex conjugate

$$E(\nu)^2 = E(\nu)^* \cdot E(\nu)$$

This product eliminates the complex components, which is why Figure 2 displays only real and positive components. This multiplication also increases the amplitude of the signals proportionally[3].

[3]To aid visualization we scale this data

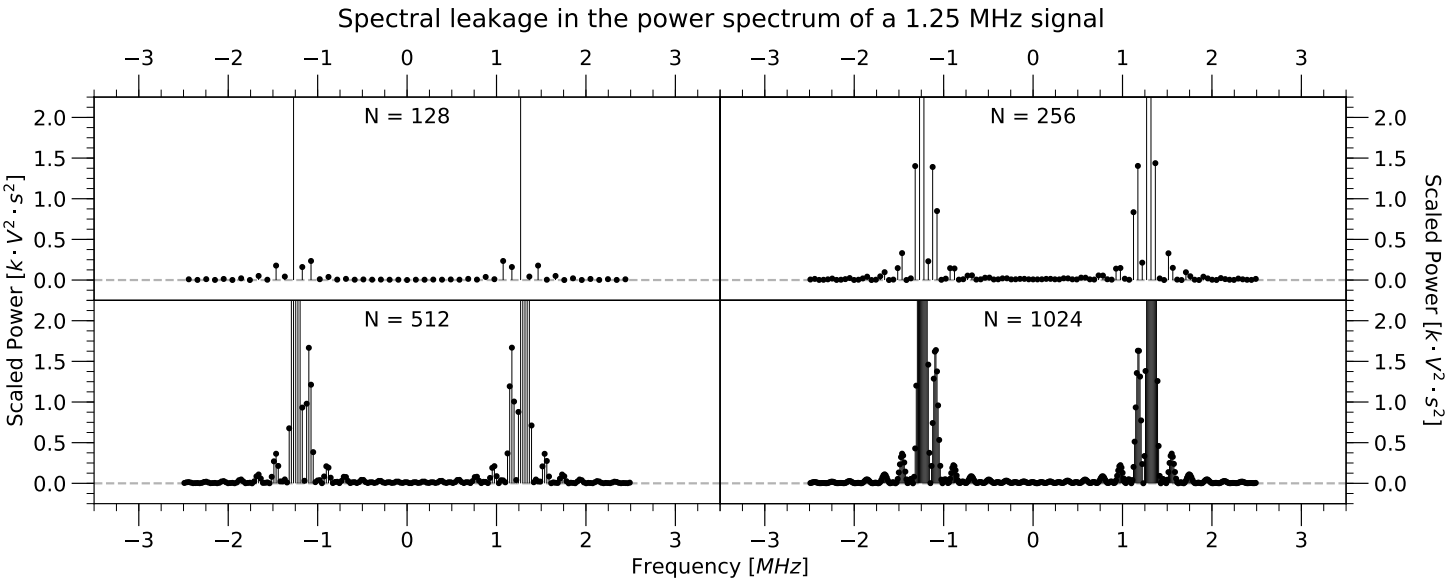

Figure 4: Increasing the number of samples reveals spectral leakage.

2.3 Leakage power

Using the dft.dft function we again compute the Fourier transform for the 1.25 MHz signal data from Figure 1. In a discrete Fourier transform, each frequency is separated by $\Delta\nu \propto 1/N$. We increase the number of samples taken, N, and decrease $\Delta\nu$.

In Figure 4 we zoom in both axes to provide an enhanced view[4]. As N is increased we observe the power spectrum spreading out and simultaneously gaining amplitude. By increasing N we reduce the size of each frequency bin in the output transform. Increasing our precision in frequency measurement is reducing our precision in time measurement, this change causes the spectral leakage seen here. This pair of variables are behaving according to Heisenberg's Uncertainty Principle. Neat.

[4]The scale factor k is the same here as in Figure 2

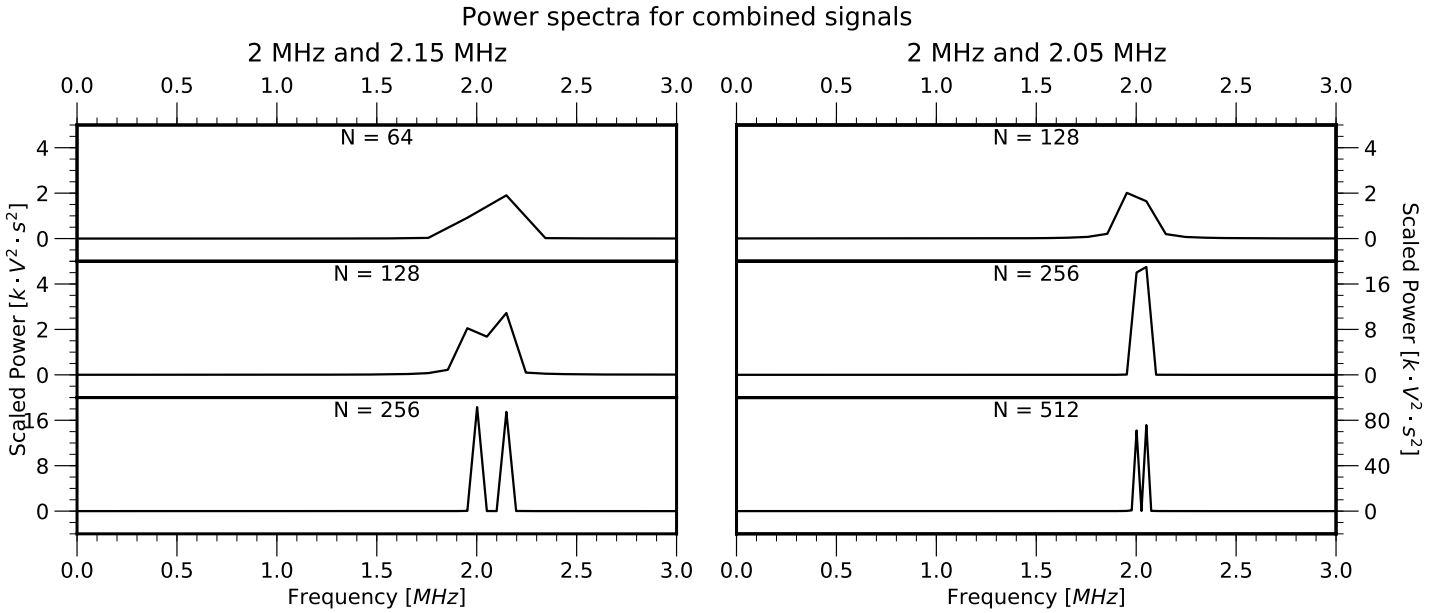

Figure 5: Increasing frequency resolution can reveal previously unnoticed information.

2.4 Frequency resolution

As discussed in Section 2.3, when we increase the value of N, the consequential reduction in the size of each frequency bin $\Delta\nu$ is also an increase in the available frequency resolution. This also increases the time interval represented in our samples. This technique can be used to reveal hidden information.

In Figure 5 we display the results of two experiments. Two signals at similar frequencies are generated and combined in a power splitter. The data is captured and transformed in our usual manner. When the frequency resolution is low, as in the upper plots, the power spectra reveal a single hump. As the resolution increases, the hump begins to resolve into two distinct peaks. When the number of samples has doubled twice, the resolution is high enough that we are able to clearly see the two peaks which represent our two signals. When the difference in the frequencies is small we have to further increase the resolution to accurately categorize our data. By doubling N we are able to discern two signals were previously only one could be seen.

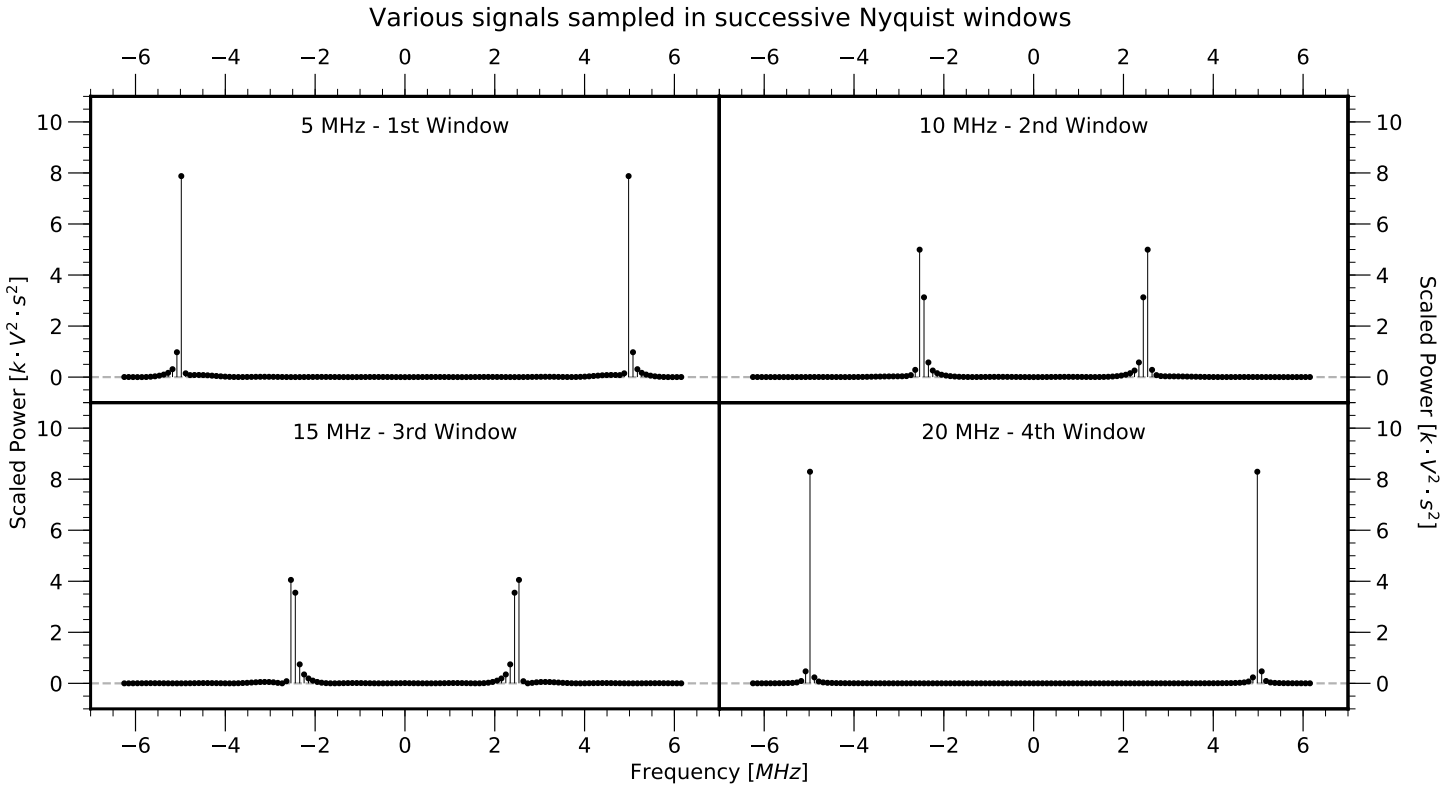

Figure 6: Nyquist Windows 3.6

2.5 Nyquist windows

In Section 1.3 we claimed that by exploiting the Nyquist criterion we could retrieve signals beyond the constrains of our sampler. We generate signals in regions that are greater than the Nyquist frequency. Each signal falls in a region that is a multiple of our Nyquist frequency. These regions are the Nyquist windows. We compute their power spectra as displayed in Figure 6[5]. Though each frequency is shown in the first window, we can extrapolate its actual frequency from its apparent frequency. For example, the 2.5 MHz signal in the upper right is in actuality a 10 Mhz signal.

[5]This portion of the lab was deeply confusing, thank you Deepthi for explaining exactly what to do

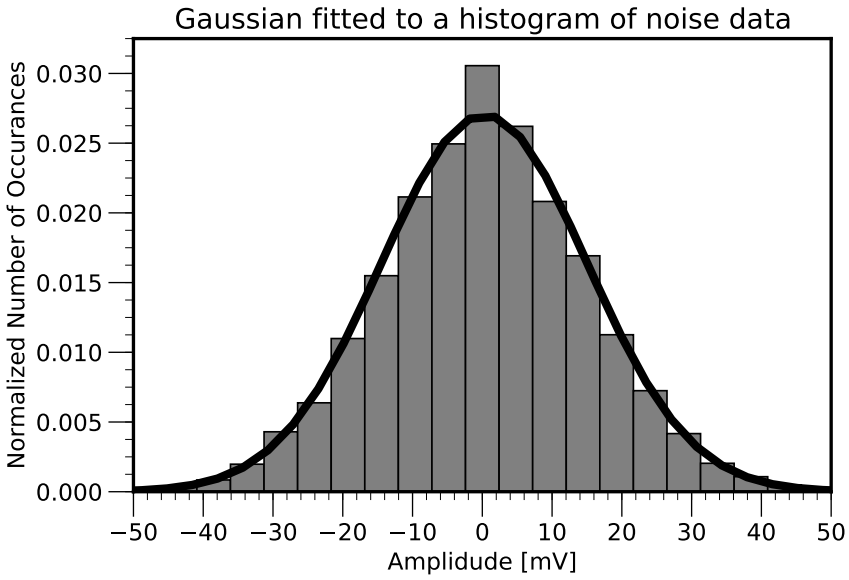

Figure 7: Confirming the Gaussian nature of random noise

2.6 Noise

2.6.1 Is it Gaussian?

The likelihood of noise in the signals we shall be analyzing in the future means we should examine its properties. We sample 32 blocks of 16000 points sourced from the the Micronetics NOD 5250 Noise Generator, passed through a Minicircuits SBP-21.4 6 MHz band-pass filter. For the first of these blocks of data, the mean voltage is 0.2 mV, the mean square voltage is 0.1 mV, and the rms voltage is 14.7 mV. We expect the noise to be Gaussian random noise, and using these values we fit a Gaussian curve to a histogram of the data as seen in Figure 7. Indeed, it is Gaussian.

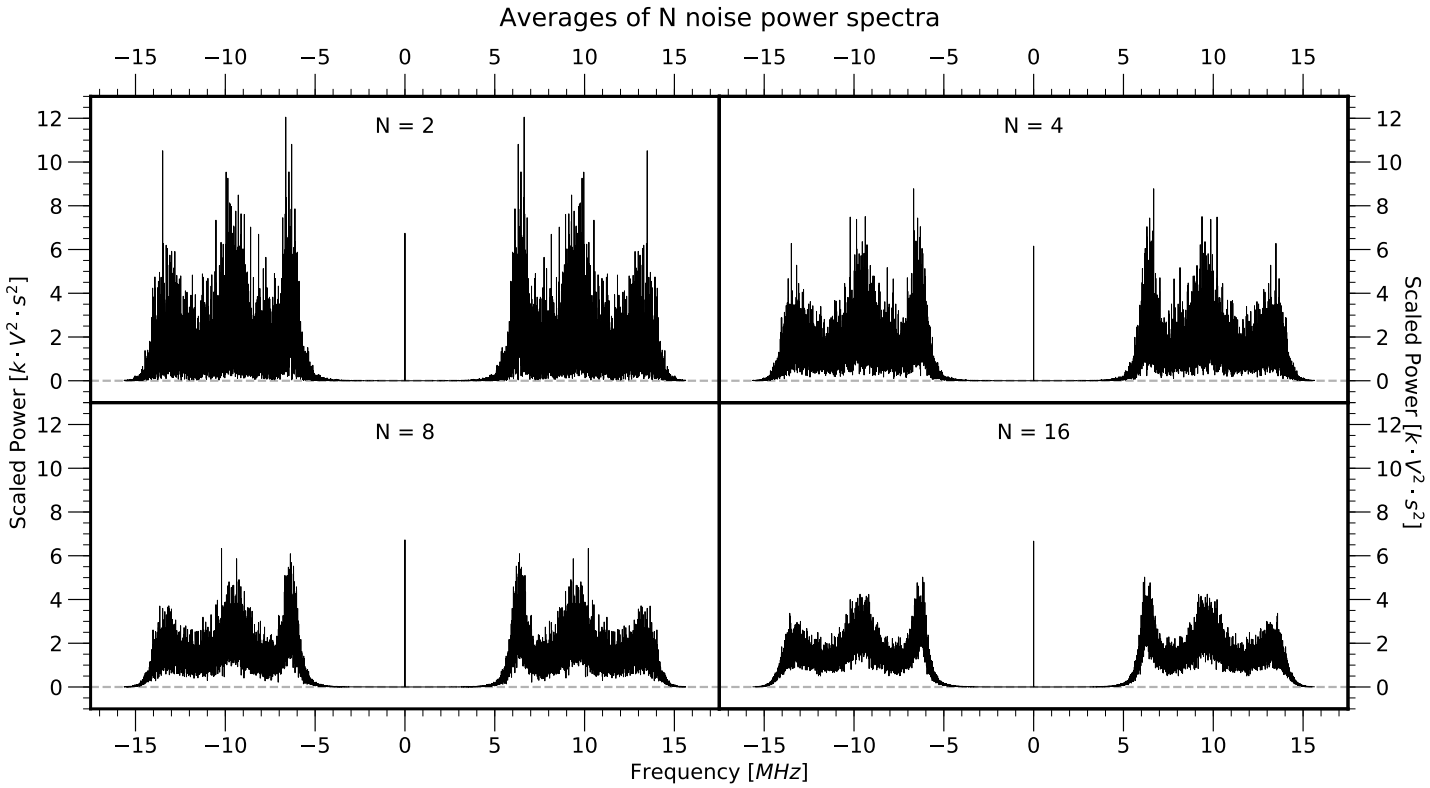

Figure 8: Attempting to determine the singal to noise ratio exponent.

2.6.2 Average Power

How does increasing the amount of data we collect affect noise in our signals? We take the average power spectrum for progressively larger blocks of noise data. In Figure 8 we show that as more blocks area added to the average, the amount of noise is reduced. This suggests that by averaging the power spectra for large numbers of blocks are able to greatly reduce, though not eliminate, the amount of noise present in our signal.

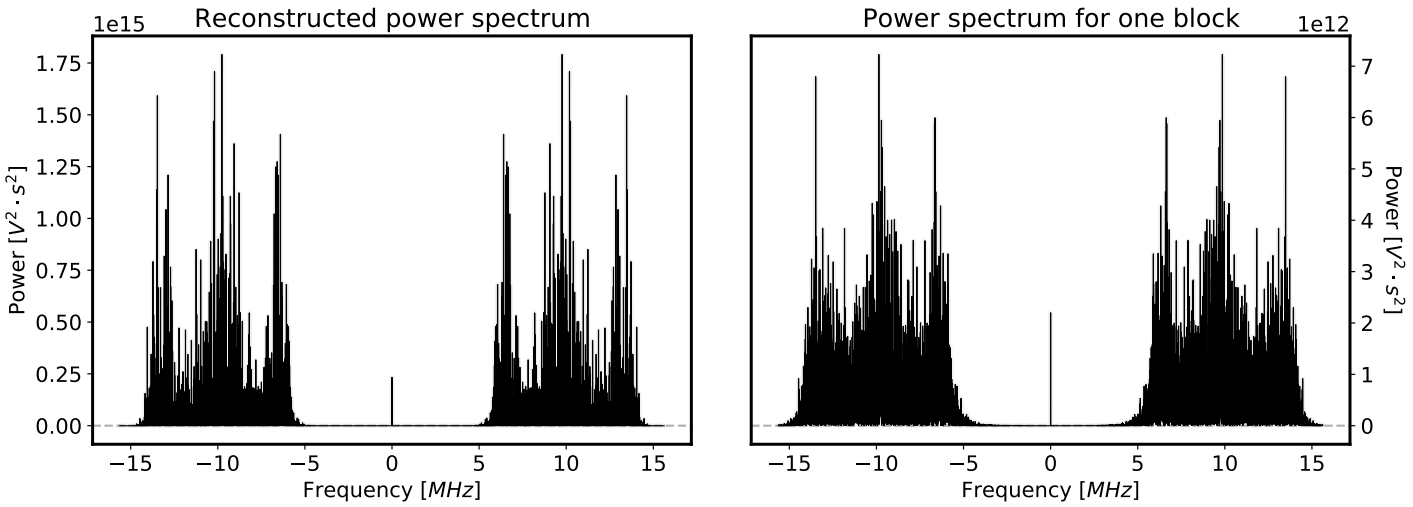

Figure 9: Attempting to determine the signal to noise ratio exponent.

2.6.3 Autocorrelation Function

The correlation theorem says that the autocorrelation of a time series should equal the power spectrum of the same signal. Using numpy, we compute the autocorrelation function for a single block and compare it to the power spectrum of the same block. Though the correlation theorem says the two should be the same, Figure 9 shows that they are only similar. Of particular interest, the scales are different by a factor of 10^3. We cannot fully explain the discrepancy at this time.

3 Mixers

Mixers are devices the combine two signals. These analog devices multiply the two signals together to produce a third signal which has data about the others encoded within it. We can use mixers to shift a signal into a frequency range that our digital sampling equipment can accurately read. Typically in a mixer the RF input is some high frequency signal, and the LO or Local Oscillator is some low frequency signal we control. We examine the properties of two types of mixers.

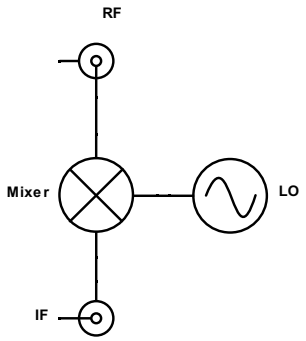

Figure 10: Double-Sideband Mixer

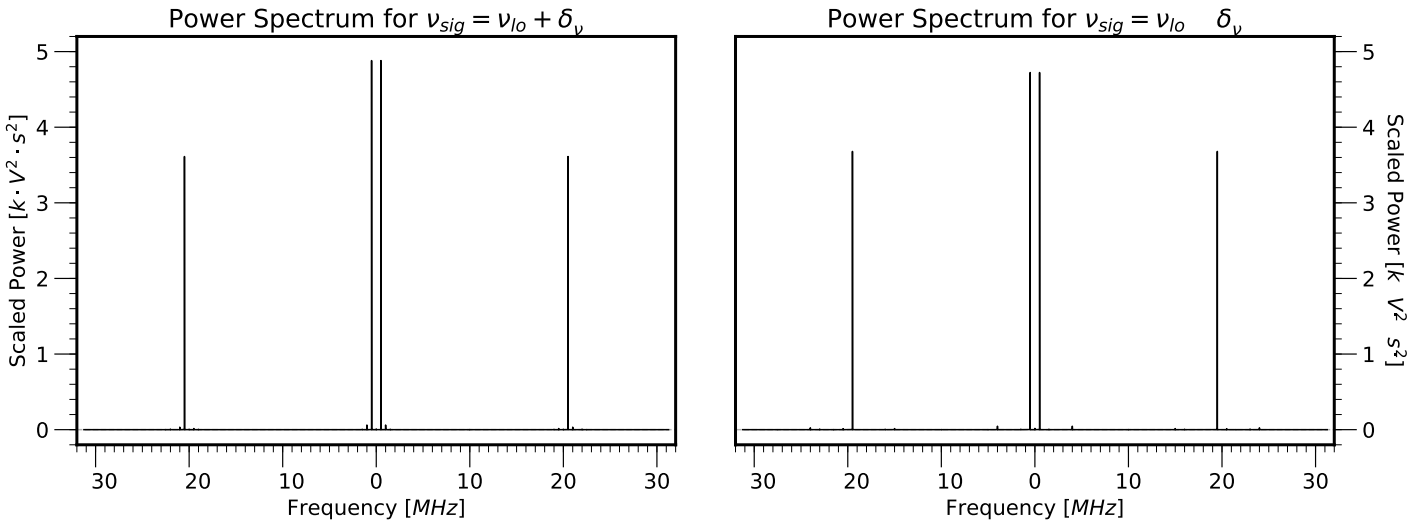

Figure 11: Power 5.1

3.1 The Double-Sideband Mixer

We construct the Double-sideband mixer in Figure 10. Our DSB uses a Mini-Circuits ZAD-1 mixer. We input two signals to our DSB, and ν_{sig} and ν_{lo}, generated with our Teledyne WaveStation 52. The two signals are in phase, $0.5V_{p-p}$ but differ in frequency by 0.5 MHz. The sampler is set to its full 62.5 MHz sample rate, and the cables in use all have lengths as equal as possible to eliminate possible phase variance. For two cases, $\nu_{sig} = \nu_{lo} \pm \delta_\nu$, we take time series data and compute their power spectra. Our ν_{sig} values were 10.5 and 9.5 MHz, with ν_{lo} fixed at 10 MHz.

In the right plot Figure 11 we see δ_ν as the large central spikes at ± 0.5 MHz. On the right side of the plot we see the combination of the two frequencies at 19.5 MHz in the upper sideband, and in the lower sideband we see the sum of the negative frequencies at -19.5 Mhz.

On the left side of 11 we see δ_ν as the large central spikes at ± 0.5 MHz. On the right side of each plot we see the combination of the two frequencies at 20.5 MHz in the upper sideband, and in the lower sideband we see the sum of the negative frequencies at -20.5 Mhz.

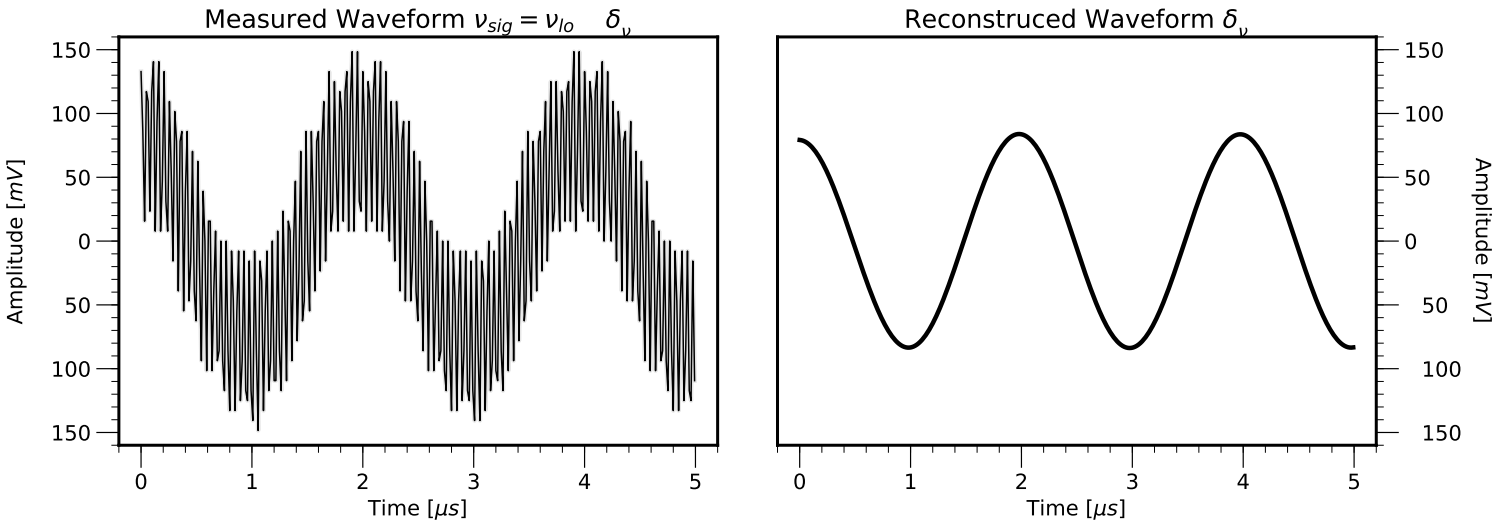

Figure 12: Waveform Reconstructed 5.1

3.1.1 Reconstructed Waveform

We filter out all but δ_ν from our DSB power spectra by setting the high frequency components to zero and compute the inverse Fourier transform using numpys fft module. This reconstructed waveform is seen in the right of Figure 12. The signal shown, δ_ν, is the beat between the frequencies of 10 MHz and 9.5 MHz. The amplitude of the measured waveform is about 30% lower than the generated signals, which we attribute to the ZAD-1[2].

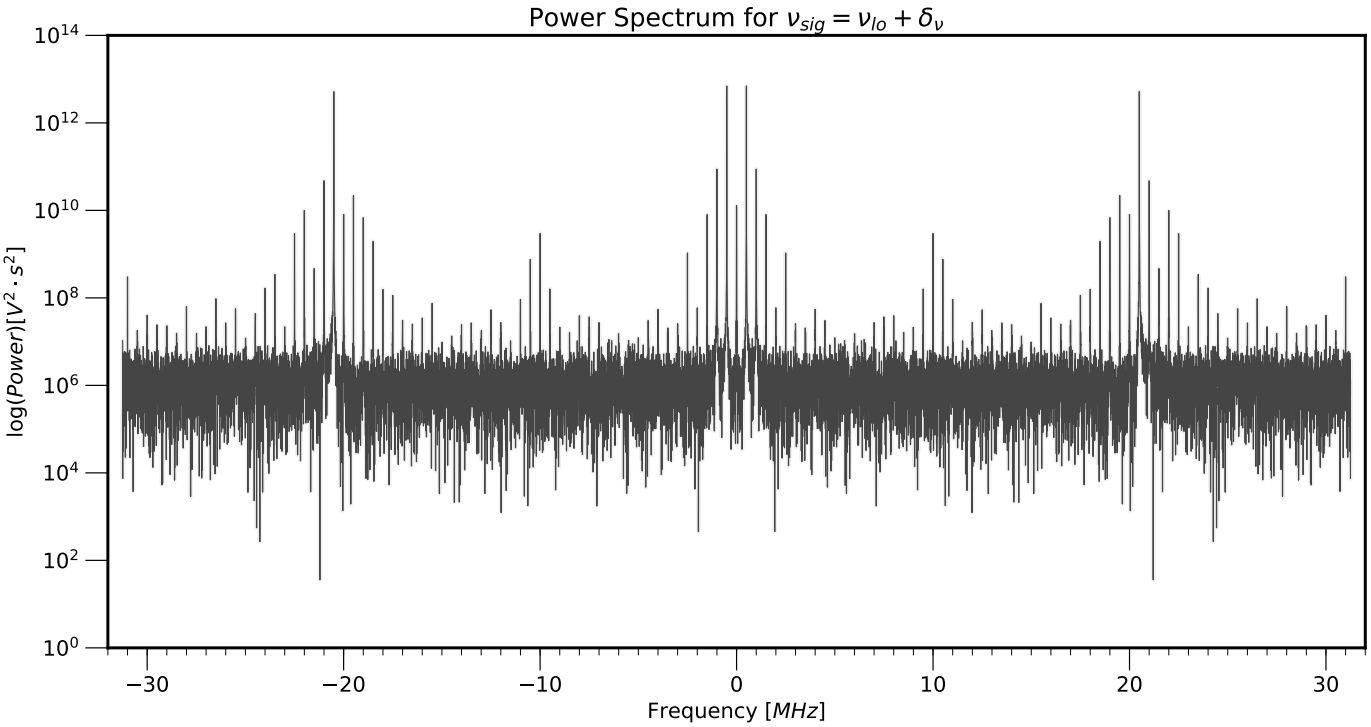

Figure 13: Logged power 5.2

3.1.2 Inter-modulation Products

Mixers are imperfect. When the two signals are combined, all the harmonics of the signals are also combined with each other. By plotting the log of the power spectrum from Figure 11 we are able to see that the clean signal we believed we had sampled is actually composed of numerous other signals. Our DSB mixer is generating intermodulation products.The large triangular shapes are the result of convolution.

3.2 The Sideband-Separating Mixer

An alternate type of mixer is the Sideband-Separating mixer, also known as the Single-Sideband Mixer. This device employs a second mixer, and it removes the upper sideband. Removing the upper sideband allows us to determine the frequency of $\delta\nu$ more accurately[6].

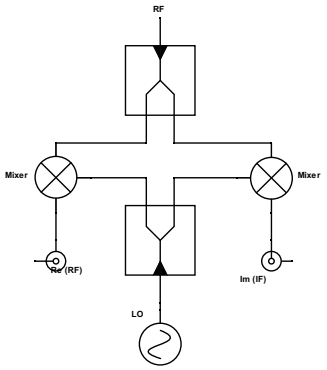

Figure 14: Single-Separating Mixer

[6]This statement may be incomplete

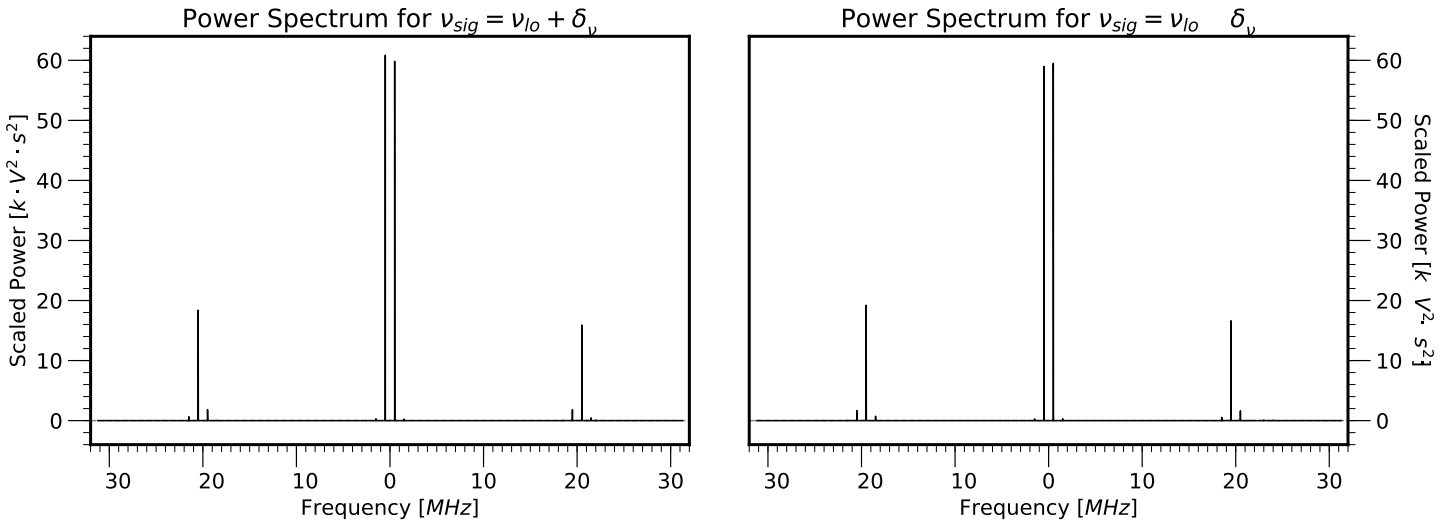

Figure 15: Power 5.3.1

3.2.1 As a Double-Sideband Mixer

We construct our Single-Separating Mixer, but manipulate its inputs so that it operates as a Double-Sideband Mixer. We feed our SSB the same signals from Section 3.1, still with zero phase difference between them. The signals are sampled as before, and the power spectra are computed. The power spectra here look largely like those in 3.1, with some more noise present. The amplitudes of $\pm\delta\nu$ are different, but operating the SSB as a DSB does not seem to have any added benefit.

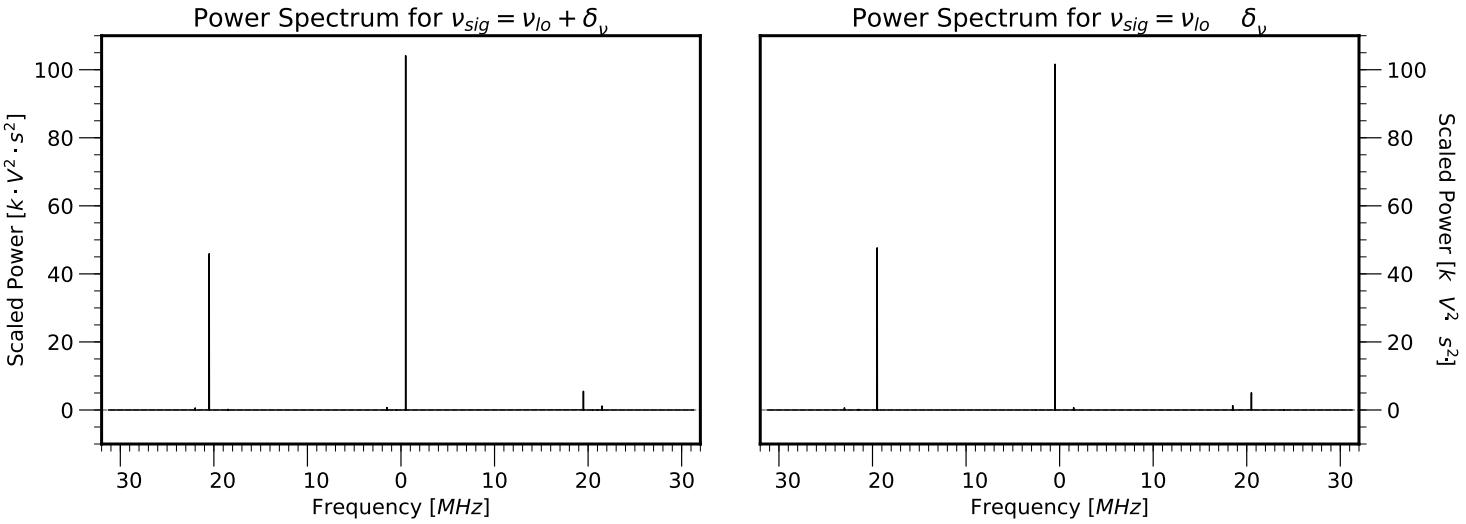

Figure 16: Power 5.3.2

3.2.2 The True Sideband-Separating Mixer

We take our Single-Separating mixer from 14 and adjust its inputs. By setting one input to be 90 degrees out of phase from the other using the signal generator, each input is complex and we operate our mixer as a true Sideband-Separating mixer. The difference from Figure 15 to Figure 16 is dramatic. The true SSB drops out the entire upper sideband, though there is some noise remaining. It is now clear which of the two plots contains the positive and negative values of δ_ν.

Conclusions

In this, our initial look into the tools of the trade of radio astronomy, we explored how to sample and analyze signals. We have shown we are able to use the laboratory equipment and the ugradio package to sample various signals. By learning how to exploit the Nyquist criterion, we have shown how to sample signals at a rate far higher than our equipments specifications. Fourier transforms provide us with a powerful tool to examine the frequency data embedded in our recorded signals, providing an important avenue of data analysis. While there is still much to learn on the topic of mixers, we are confident we can construct the necessary devices and interpret their outputs in the future. Our most troublesome part of this lab were the difficulties we sustained in understanding what exactly was desired of us in the Nyquist windows and autocorrelation sections of the writeup. Though we have examined these sections repeatedly, we feel a review of the content would be beneficial.

Distribution of Effort

In any group effort, the distribution of work is uneven. In this case that unevenness represented itself in a particularly beneficial manner. Each group member gravitated to an area where there natural skills shone, as well as applying themselves to the group tasks as a whole. Amanda repeatedly reviewed the lab writeup, keeping the group on task and ensuring we all understood the required procedures, in addition to compiling a spreadsheet of our collected data. Steve has a natural ability with electrical devices, and in addition to performing the necessary setups he made sure the group knew the function of each component. I have a knack for plots with a decent knowledge of Pythons matplotlib package, so I took it upon myself to compile our group presentations. Hayley focused on the analysis of the data, transmitting multiple data sets to the group. While they may have had a particular aptitude for one component or another, each group member fully participated in all areas of this lab. For our reports each member created their own notebooks, working through the analysis and generating their desired plots from the raw data.

Location of Data and Analysis Notebooks

If you would care to, our data is available for perusal in my Documents directory on the Radio Laboratory network. The directories which end with an X contain data in various formats, as well as all the notebooks used in the generation of the figures used in this report. Note that these notebooks were written on a system using Python 3 which may cause minor compatibility issues. The notebooks which employed the `ugradio` package are in a separate folder not marked with an X. These notebooks were used for data collection and generation in addition to rudimentary analysis.

Acknowledgements

A portion of the Fourier transform analysis was sourced from the lab writeup[1], or from lecture. The other members of my group were each instrumental in their own unique way in furthering my understanding of this material. I would also like to single out one of our GSI's, Deepthi, for helping me work through the Nyquist windows and the inverse Fourier transforms. And a special thanks to Professor Parsons for patiently answering my questions.

References

[1] Exploring digital sampling, fourier transforms, and both dsb and ssb mixers. https://github.com/AaronParsons/ugradio/blob/master/lab_mixers/allmixers.pdf. Accessed: 2018-02-05.

[2] Zad-1 specification sheet. https://www.minicircuits.com/pdfs/ZAD-1+.pdf. Accessed: 2018-02-06.